Noise cancelling of MRS signals combining model-based removal of powerline harmonics and multichannel Wiener filtering

Jakob Juul Larsen,[1] Esben Dalgaard[2] and Esben Auken[2]

[1]*Department of Engineering, Aarhus University, Finlandsgade 22, 8200 Aarhus N, Denmark. E-mail: jjl@iha.dk*
[2]*Hydrogeophysics Group, Department of Geoscience, Aarhus University, Denmark*

SUMMARY

The fidelity of magnetic resonance sounding signals is often severely degraded by noise, primarily electrical interference from powerline harmonics and short electromagnetic discharges. In many circumstances, the noise originates from multiple sources. We show that noise cancelling can be improved if the multiple origins of noise are taken into account. In particular, a method is developed where powerline harmonics are efficiently removed through a model-based approach. Subsequently, standard multichannel Wiener filtering can be used to provide a further noise reduction. The performance of the method depends on the distribution of noise on the particular site of measurement. Simulations on synthetic signals embedded in real noise recordings show that the combined approach can improve the signal-to-noise ratio with an accompanying improvement in retrieval of model parameters.

Key words: Time-series analysis; Fourier analysis; Hydrogeophysics.

1 INTRODUCTION

A common problem for most geophysical measurements performed in the proximity of human activities, for instance, seismic, seismo-electric, induced polarization and magnetotelluric measurements, is the man-made noise imposed on the measurements. Magnetic resonance sounding (MRS) signals are also susceptible to such noise and the measured signals are normally severely distorted by electrical interference from powerlines. Electrical interference from powerlines in geophysical measurements is a well known and studied problem that has been addressed by a number of authors (e.g. Butler & Russell 1993, 2003; Xia & Miller 2000; Butler 2001). Other noise sources, such as short electrical discharges (called spikes) of both natural and man-made origin, can also have a detrimental effect on the quality of the data. In the case of MRS recordings, noise is a serious problem. The direct measurements of water content that the MRS technique can provide, are often needed in urban areas where they are also most likely to be influenced by noise. To recover the signals of interest, the electrical interference from powerlines and other noise contributions must be removed from the recordings with appropriate hardware- or software-based signal processing.

The development of increasingly sophisticated MRS instruments has progressed in two stages. The first generation of MRS instruments was single-loop systems where the same loop was used for excitation and recording of the MRS signal (e.g. Legchenko *et al.* 2002). Electrical interference from powerlines occurs in the form of harmonics of the fundamental powerline signal. The interference can be removed by different methods. For instance, Legchenko & Valla (2003) compared the use of block subtraction, sinusoid subtraction and notch filtering for a single-channel system. However,

notch filtering can be problematic. The filter will affect the MRS signal if the Larmor frequency is close to one of the powerline harmonic frequencies and further, the presence of spikes in the signal will excite the filter and cause it to ring with a subsequent signal degradation. In their study, Legchenko and Valla found that the efficiency of the different noise filtering methods was site-dependent reflecting the different noise conditions at the specific sites.

The second generation of MRS instruments consists of multichannel systems (Walsh 2008; Dluglosch *et al.* 2011). One loop is again used for excitation and recording of the MRS signal. In addition, a number of reference loops, appropriately distanced from the primary loop, record the local noise conditions simultaneously with the MRS signal. The noise in the primary loop and the reference loops are correlated and, through filtering, the signals from the reference loops can be transformed into an estimate of the noise in the primary loop. The estimate is subtracted from the primary loop signal leaving only the desired signal (Walsh 2008; Mueller-Petke & Yaramanci 2010; Dalgaard *et al.* 2012). However, as will be demonstrated below, this approach is not always optimum. The filters cannot be optimized simultaneously for all noise sources but are effectively an average over all noise sources. The consequence of this averaging is that the noise cancelling is reduced when several noise sources are present.

The goal of this paper is to address the problem of multiple noise sources. We discuss the noise characteristics of typical MRS recordings and the appearance of multiple noise sources. We propose to use a model-based approach similar to sinusoid subtraction, to remove powerline harmonics from all channels. Through this approach, one specific component of noise is efficiently removed. Subsequently, standard multichannel noise cancelling can be
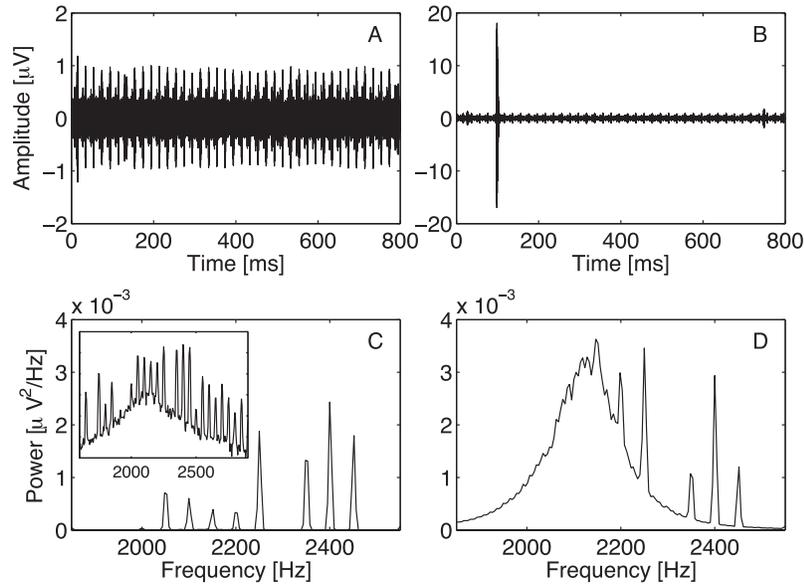
Figure 1. Two noise-only records in the time (top panels) and frequency (bottom panels) domains. Left-hand panels: the noise is primarily near-stationary powerline interference. Right-hand panels: an intense spike is present and dominates the temporal and spectral view. The inset in panel (c) shows the frequency spectrum on a logarithmic scale.

applied. The model-based noise cancelling approach is analysed and optimized using synthetic MRS signals superimposed on real MRS noise records with special emphasis on the case where one powerline harmonic frequency is close to the Larmor frequency. Examples of subsequent noise cancelling are given and discussed. We show that our method can lead to an overall improved noise cancelling and a corresponding improved retrieval of the desired MRS signal.

2 NOISE IN MRS RECORDINGS

As discussed above, MRS signals are primarily distorted by interference from powerline harmonics and spikes. Two typical examples of noise imposed on a MRS recording are shown in Fig. 1 in both the time and frequency domain. The signals were recorded without a prior excitation pulse, that is, the records contain only noise and no NMR signal. The system used for the measurements is a four-channel Numis Poly from Iris Instruments (France). The corner-to-corner distance between the 100×100 m, 1-turn square loop primary coil and the 10×10 m, 7-turn square loop, reference coils was approximately 80 m with similar distances between the reference coils. The signals from all coils are bandpass filtered before sampling. The centre frequency of the bandpass filter can be adjusted to the Larmor frequency at the measurement site and the bandwidth of the filter is 150 Hz. All channels are sampled at a frequency of $f_s = 19.2$ kHz. The data are recorded at Odder, Denmark.

The example data series shows a repeating pattern with a peak amplitude of approximately 1 μV (Fig. 1a). The origin of this pattern is found in the corresponding power density spectrum (Fig. 1c). Here, it is evident that the power is primarily located at a number of discrete frequencies corresponding to high-order harmonics of the fundamental 50 Hz powerline frequency. The pattern of the time-series is caused by the sum of these sinusoidal signals repeatedly adding up constructively and destructively. Under most circumstances, many, both odd and even, high-order harmonics are excited. The harmonic signal resides on top of a broad spectral peak. This peak is caused by a combination of broad-band stationary and impulsive noise filtered by the bandpass filter.

The second example is from Risby, Denmark (Fig. 1b). The separation between all loops is again approximately 80 m corner-to-corner. In this case, the recording is disturbed by an intense spike with a peak amplitude of almost 20 μV and a duration of a few milliseconds. Away from the spike, the repeating pattern with an amplitude of 1 μV is still observed. The influence of the intense spike on the corresponding power density spectrum is pronounced (Fig. 1d). The spectrum, calculated on the entire 800 ms time-series, is dominated by one broad feature caused by the short spike and the contribution from the powerline harmonics is much less. The spectral shape is mainly determined by the bandpass filter in the instrument, as a short spike corresponds to a near impulsive excitation of the bandpass filter. Similarly, the temporal profile of the spike is shaped and elongated by the impulse response of the bandpass filter.

When more than one noise source contributes with spikes, for example, two electrical fences at different directions and distances from the MRS instrument the complexity of the recorded time-series is increased (Fig. 2). In this example, the time-series are again recorded without prior MRS excitation and are therefore noise-only records. The four time-series consisting of the primary channel and the three reference channels are recorded simultaneously. Two spike events, labelled A and B, are observed. The two spike events are clearly different, as seen by the different amplitudes in the channels. The A-spike is recorded with an almost identical amplitude in the primary and reference 2 channel, but the amplitude of the B-spike differs by a factor of 2 between the same two channels. This observation is consistent with spikes A and B coming from two different sources and it has profound consequences for the noise cancelling of multichannel MRS signals. In multichannel filtering, the reference signals are filtered into a replica of the noise in the primary channel and subtracted from this record. However, the filters that are optimum for cancelling the A-spike are not sufficient for cancelling the B-spike nor the powerline harmonics and vice versa. In practice, the filters are determined as a least mean square average over all noise sources and the result is therefore that no noise component is efficiently cancelled when noise from several sources
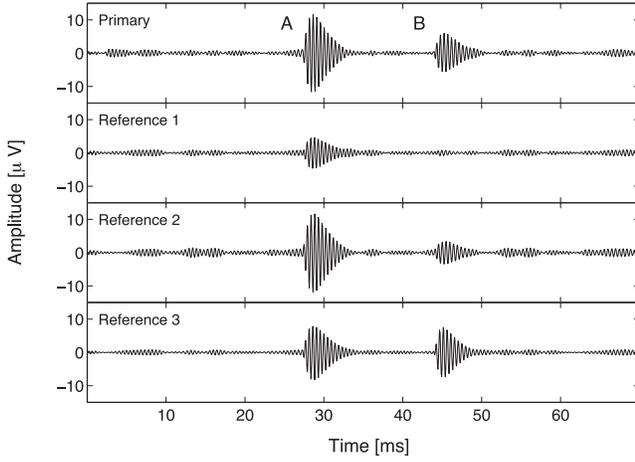
Figure 2. Short excerpt from a noise-only time-series showing the simultaneously recorded signal in the primary channel (top) and reference channels 1–3 (below). Two different spike events at A and B are observed.
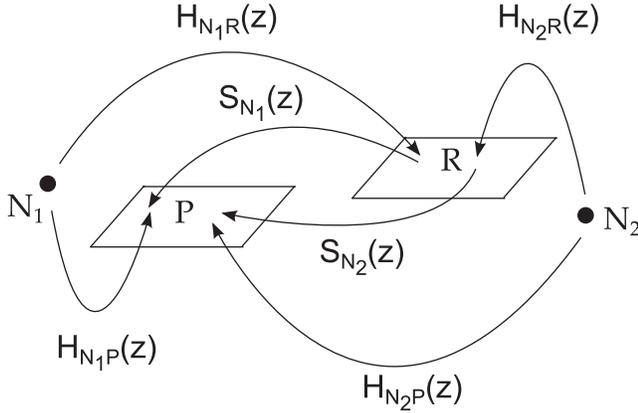
Figure 3. Schematic overview of the two noise sources problem. The signals from the two different noise sources N_1 and N_2 are recorded by the primary receiver (P) and a reference receiver (R) but pass through four different transfer functions $H_{N_1 P}(z)$, $H_{N_1 R}(z)$, $H_{N_2 P}(z)$ and $H_{N_2 R}(z)$ before they reach the detectors. Due to differences in the four transfer functions, the optimum transfer functions for noise cancelling of the two noise sources $S_{N_1}(z)$ and $S_{N_2}(z)$ are not equal.

is simultaneously present. This argument can be mathematically stated. For simplicity, consider a two-channel MRS system with a primary channel (P) and a reference channel (R) and two noise sources N_1 and N_2 (Fig. 3). The signal from N_1 will be recorded in the primary channel and the reference channel. The signal pathways from the N_1 noise source to the two receivers are not identical due to the different distances from the noise source to the coils, the size, geometry and orientations of coils and the differences in receiver electronics. The two signal pathways are modelled as discrete-time transfer functions $H_{N_1 P}(z)$ and $H_{N_1 R}(z)$. The optimum digital filter for cancelling the N_1 noise, $S_{N_1}(z)$, should make the path from the noise source N_1 to the reference channel and further on to the primary channel identical to the direct path from the noise source to the primary channel, that is,

$$H_{N_1 P}(z) = S_{N_1}(z) H_{N_1 R}(z) \iff S_{N_1}(z) = \frac{H_{N_1 P}(z)}{H_{N_1 R}(z)}. \tag{1}$$

The same argument applies to the second noise source and the optimum filter for cancelling the second noise source is therefore

$$S_{N_2}(z) = \frac{H_{N_2 P}(z)}{H_{N_2 R}(z)}. \tag{2}$$

As seen $S_{N_1}(z)$ and $S_{N_2}(z)$ are not identical as tacitly assumed in the standard method of noise cancelling of multichannel MRS signals (Walsh 2008; Mueller-Petke & Yaramanci 2010; Dalgaard *et al.* 2012). To improve on this matter, more advanced signal processing schemes must be devised where the contributions from different sources are thoroughly separated and independently cancelled.

3 MODEL-BASED SIGNAL PROCESSING

Our approach for improved noise cancelling is based on utilizing prior knowledge of the powerline interference. The interference is a sum of sinusoidal signals with frequencies given by an integer multiple of the common fundamental powerline frequency, but with independent amplitude and phase of each sinusoidal component. If the fundamental frequency and the amplitude and phase of all components can be correctly determined, a mathematical model of the powerline interference can be constructed and subtracted from the noise record.

The signal recorded in the primary channel, $p(k)$, sampled at time k, is described by the model

$$p(k) = FID(k) + h_p(k) + spikes_p(k) + N_p(k). \tag{3}$$

Here, $FID(k)$ is the desired free induction decay signal from the subsurface protons. The powerline interference in the primary channel is denoted by $h_p(k)$. All spikes present in the primary channel signal are collectively described by the term $spikes_p(k)$. The last term $N_p(k)$ denotes all other noise components present in the primary channel signal originating from broad-band noise filtered through the bandpass filter, harmonic components unrelated to the powerline frequency, receiver electronic noise, etc.

The powerline interference is modelled as

$$h_p(k) = \sum_m A_m^p \cos\left(2\pi m \frac{f_0}{f_s} k + \phi_m^p\right). \tag{4}$$

Here, f_0 is the common fundamental powerline frequency, f_s denotes the sampling frequency and A_m^p and ϕ_m^p are the amplitude and phase of the mth harmonic component. The summation over m extends over all excited harmonics, typically $1 \leq m \leq 100$.

Similarly, the signals in the three reference channels are modelled as a sum of the powerline interference, spikes and remaining noise.

$$r_i(k) = h_i(k) + spikes_i(k) + N_i(k) \quad i = 1, 2, 3. \tag{5}$$

The reference channels are assumed to be free of contamination from free induction decay signal. The powerline interference is again modelled as a sum of sinusoidal signals with channel-dependent amplitude and phase for each component:

$$h_i(k) = \sum_m A_m^i \cos\left(2\pi m \frac{f_0}{f_s} k + \phi_m^i\right). \tag{6}$$

In the above models, it is assumed that the fundamental powerline frequency and the amplitude and phase of each component are constant. However, the powerline frequency is constantly fluctuating due to changes in demand and supply of power. Due to the non-linear processes generating the high-order powerline harmonics, the amplitudes and phases of each sinusoidal component are also time variant. For short periods of time, less than a few seconds,

the powerline frequency, amplitudes and phases can be assumed constant and the modelling approach is viable, but care must be exercised to validate the model.

3.1 Removing powerline interference

The determination of the model parameters A_m, ϕ_m and f_0 in eqs (4) and (6) is a non-linear optimization problem. The problem is simplified through the standard approach of rewriting the cosine terms as

$$A_m \cos\left(2\pi m \frac{f_0}{f_s}k + \phi_m\right) = \alpha_m \cos\left(2\pi m \frac{f_0}{f_s}k\right)$$

$$+ \beta_m \sin\left(2\pi m \frac{f_0}{f_s}k\right), \quad (7)$$

where the variables are related as

$$A_m = \sqrt{\alpha_m^2 + \beta_m^2} \quad (8)$$

and

$$\tan(\phi_m) = -\frac{\beta_m}{\alpha_m}. \quad (9)$$

After the rewrite, the only non-linear parameter is f_0. The value of f_0 is known in advance to be constrained to a narrow range around 50 Hz. A simple method for determining the model parameters is therefore to treat f_0 as a parameter and solve the linear equations with a standard least-squares approach (Lay 2012) for several f_0 values in this range and locate the optimum. For numerical efficiency, a two-step approach can be employed where only a handful of well-excited harmonics are used in the first step to narrow the f_0 search range. In the second step, the parameters of all harmonics are then determined.

Spikes can influence the determination of the model parameters, in particular, large spikes can saturate the detector system and the recorded signals will be clipped. To avoid this problem, the segments of a time-series containing spikes are identified and discarded during the modelling process (Dalgaard *et al.* 2012).

Several conclusions can be drawn from a plot of the residual power in the signal, that is, after subtraction of the harmonic model, as a function of the assumed value of f_0 (Fig. 4). The time-series used in this example is a noise-only record of 1 s duration. A clear minimum is seen at 50.016 Hz. The minimum can be located to within approximately 1 mHz and deviations of the fundamental powerline frequency of just a few millihertz from the optimum value will reduce the noise cancelling efficiency.

It is instructive to compare the time-series and power spectrum of the noise-only record before and after model-based removal of the powerline harmonics (Fig. 5). In this case, more than 96 per cent of the noise power in the recorded signal is modelled as a harmonic signal and removed. The power spectrum shows that all harmonics have been efficiently removed. The same is evident in the time-series where the repeating pattern has disappeared. Importantly, the time-series now also reveals the presence of a number of small spikes that were masked by the powerline interference.

3.2 Optimization of powerline interference removal

An important issue to address for this noise cancelling algorithm is the resemblance between the MRS signal oscillating at the Larmor frequency and the powerline harmonics when one of the harmonics is oscillating at a frequency close to the Larmor frequency. When
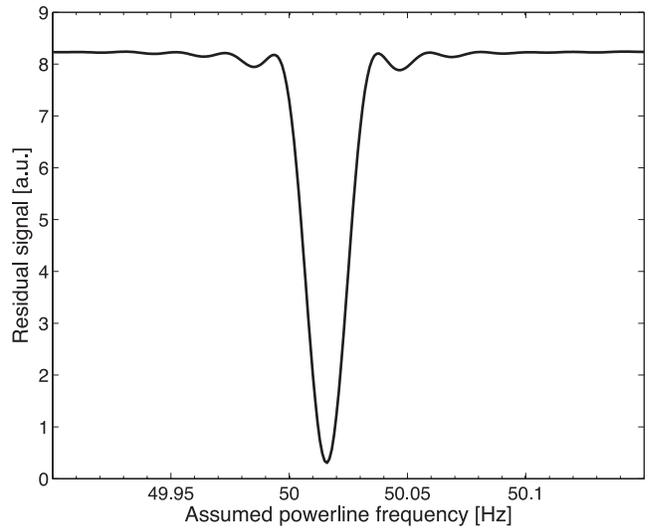
Figure 4. Plot of the residual signal power after modelling and removal of powerline harmonics at the assumed powerline frequency. The powerline frequency must be determined to within approximately 1 mHz for optimum noise removal. The nominal powerline frequency in Denmark is 50 Hz but the instantaneous value is constantly fluctuating.

the frequency difference is small, the algorithm cannot distinguish between MRS signal and noise. This implies that the MRS signal can be distorted in the noise cancelling processing with corresponding errors in the subsequent inversion of the data. To address this issue and establish the limitations and best practice for model-based powerline harmonics removal, a number of numerical experiments have been performed.

The numerical experiments are based on embedding a synthetic signal given by

$$s(k) = s_0 \cos\left(2\pi \frac{f_1}{f_s}k + \phi\right) e^{-kT_s/T_2^*} \quad (10)$$

in real noise-only records recorded at different sites. In eq. (10), the amplitude and decay time of the FID signal is denoted by s_0 and T_2^*, the phase of the retrieved signal enters as ϕ, f_1 denotes the Larmor frequency and $T_s = 1/f_s$. The noise is cancelled using different settings and the retrieved signal is compared with the known synthetic signal. The synthetic signal in eq. (10), consisting of a mono-exponential decay, is an oversimplification compared to real multiexponential MRS signals. However, the simplification allows for an easy interpretation of results while it captures the nature of the physical signal. For the experiments presented here, the synthetic signal was embedded in 32, 1 s duration noise-only records. The properties of the synthetic signal are $s_0 = 200$ nV and $T_2^* = 150$ ms. The synthetic signal is recovered by removing spikes, applying the harmonic subtraction followed by a second spike removal and stacking of the records. The MRS signal is then estimated from the average stack using the envelope detection procedure described in Dalgaard *et al.* (2012) and fitting the envelope to the mono-exponential decay. The procedure is repeated with different Larmor frequencies ranging from 2075 to 2125 Hz.

Three different methods of harmonic subtraction have been employed and the efficiency of the methods is compared by the root mean square error (RMSE) between the fit to the exponential model and the noise-cancelled data (Fig. 6). With the first method, shown with triangles, the harmonics from 1 to 100 are removed, based on fitting the harmonic model to the entire 1 s time-series. The RMSE is increased when the Larmor frequency of the synthetic signal is
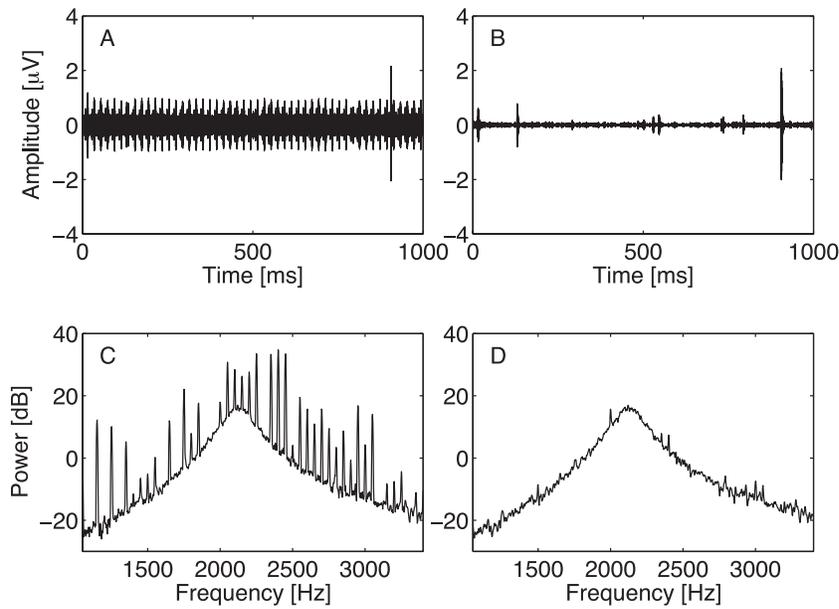
Figure 5. Time-series and spectra of a noise-only record before (a and c) and after (b and d) model-based subtraction of powerline harmonics. The model is determined from the entire time-series and include all harmonics from 1 to 100. After subtraction of powerline harmonics, the presence of a number of small spikes is evident in b). These spikes are also present in the time-series in (a), but masked by powerline harmonic noise.
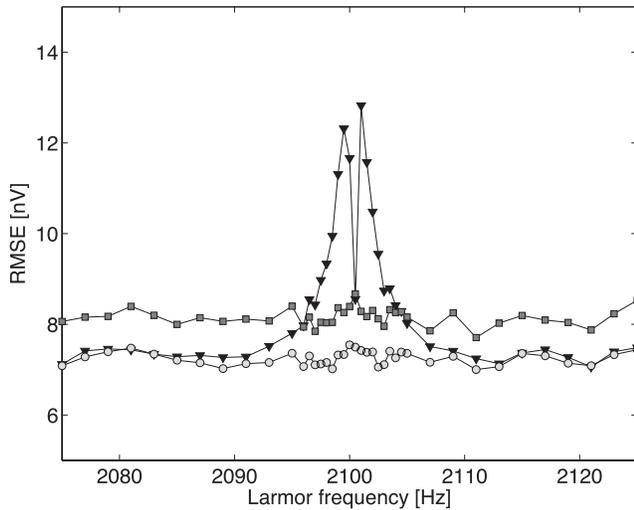
Figure 6. Plot of the root mean square error (RMSE) between the fitted exponential model and the noise cleaned data as a function of the Larmor frequency of the synthetic MRS signal in the vicinity of the 42nd powerline harmonic at 2100 Hz. Black triangles display the RMSE when the harmonic model is fitted to all harmonics and the entire time-series. Dark grey squares display the RMSE for a harmonic model fitted to all harmonics on the last half of the time-series and extrapolated. Light grey circles display the RMSE for a harmonic model where all but the 42nd harmonic at 2100 Hz are fitted on the entire time-series. The 42nd harmonic is fitted on the last half of the time-series and extrapolated.

within approximately ± 7 Hz of the 42nd powerline harmonic at 2100 Hz. Right at 2100 Hz, the peak in RMSE experiences a dip. Similar problematic behaviour is also evident in the amplitude of the fitted model (Fig. 7). The amplitude is greatly reduced in the vicinity of 2100 Hz where the MRS signal is mistaken for noise. A similar distortion of the fitted T_2^* parameter, not shown, is also found. In the second method, shown with squares, the harmonic model is fitted on the harmonics from 1 to 100 on the last 500 ms of the times-series where the MRS signal is vanishingly small and
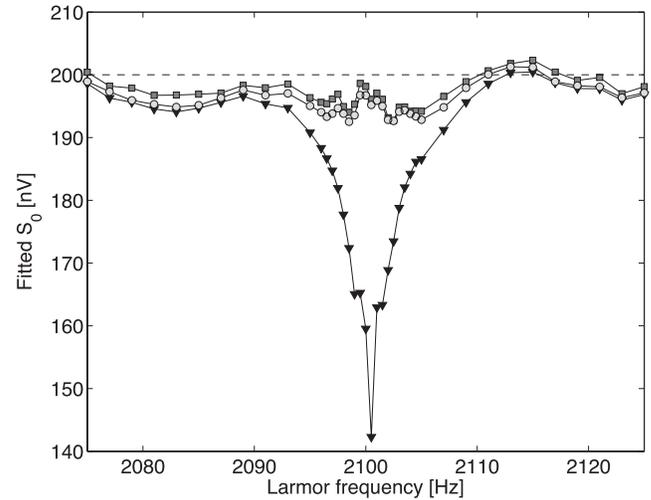
Figure 7. Plot of the amplitude, s_0, of the fitted exponential decay as a function of the Larmor frequency of the synthetic MRS signal in the vicinity of the 42nd powerline harmonic at 2100 Hz. Black triangles display s_0 when the harmonic model is fitted to all harmonics and the entire time-series. Dark grey squares display s_0 for a harmonic model fitted to all harmonics on the last half of the time-series and extrapolated. Light grey circles display s_0 for a harmonic model where all but the 42nd harmonic at 2100 Hz are fitted on the entire time-series. The 42nd harmonic is fitted on the last half of the time-series and extrapolated.

the model is extrapolated to the first 500 ms of the time-series. The result is that the RMSE is unaffected when the Larmor frequency is close to or on top of the powerline harmonic frequency and similarly important, the fitted amplitude is also unaffected. However, the RMSE is increased away from 2100 Hz due to the lower number of datapoints used in the fit and the extrapolation of the model. In the third method, shown with circles, this problem is remedied by modelling and removing all harmonics from 1 to 100, except for the 42nd at 2100 Hz, on the entire time-series. The 42nd harmonic is subsequently removed with the powerline frequency found using all

the other harmonics fitted to the entire time-series and its amplitude and phase based on fitting the model of the 42nd harmonic the last 500 ms of the time-series and extrapolating to the first 500 ms. Using this method, the RMSE is reduced and the amplitude and decay parameters are retrieved with an uncertainty of less than 5 per cent.

The methods have been tested on a number of noise records from different sites and with different parameters of the synthetic signal. Similar conclusions are achieved in all instances: all harmonics except the one close to a Larmor frequency can be efficiently removed by fitting to the entire time-series. The harmonic close to the Larmor frequency can subsequently be removed in a second step by fitting the amplitude and phase on the last part of the time-series where the MRS signal has decayed. This two-step method is used in the following sections of this paper. Numerical experiments on time-series with durations from 250 ms to 1 s have shown efficient suppression of powerline interference without distortion of the MRS signal. It should be noted that the performance of the method will degrade if the fundamental frequency of the powerline harmonics or the excitation of individual harmonics change significantly within a measurement. This is seen as residual signal at the powerline harmonic frequencies after the removal process (Butler 2001).

Figure 8. Plots of the multiple coherence function $|\gamma_{p:r}(f)|^2$ measured at three sites with different noise characteristics. The multiple coherence function is calculated after powerline harmonics have been removed. (a) Odder I (low multiple coherence). (b) Odder II (medium multiple coherence) and (c) Kasted (high multiple coherence).

4 MULTIPLE COHERENCE MEASUREMENTS

Following subtraction of powerline interference in the primary and reference channels, it is sometimes possible to remove remaining noise through additional multichannel Wiener filtering. As discussed above, this will not be successful if the remaining noise originates from multiple sources that warrant independent filtering of each source.

The maximum effectiveness of an additional Wiener filter can be quantified by measuring the multiple coherence function between the primary channel and the three reference channels, $|\gamma_{p:r}(f)|^2$. The multiple coherence function provides a frequency-resolved measurement of the linear relationship between the primary channel and the multiple reference channels. In particular, the multiple coherence function appropriately accounts for the partial correlation between signals in the reference channels which is not possible with the ordinary coherence function (Bendat & Piersol 2010). The linear relationship is quantified by a number between 0 and 1, with 0 indicating no relationship and 1 indicating a complete linear relationship. The multiple coherence function is calculated on a stack by stack basis and averaged to show the mean value. The maximum additional noise attenuation at a given frequency, expressed in dB, by a multichannel Wiener filter is given by

$$\text{attenuation}(f) = -10 \log_{10} \left(1 - |\gamma_{p:r}(f)|^2\right). \tag{11}$$

Thus, for an efficient additional noise cancelling, the multiple coherence function should take on high values in the spectral region around the Larmor frequency where the hardware bandpass filter of the Numis Poly is inefficient in rejecting noise.

The multiple coherence function is very site-dependent after model-based removal of powerline harmonics (Fig. 8). In panel A, a noise-only measurement from Odder, 20 km south of Aarhus, Denmark, is shown. The data were recorded in the summer time and this site was found to be rich in both powerline interference and spikes. In the most important region around the bandpass filter from 2 to 2.3 kHz, the value of the multiple coherence function is approximately $0.15–0.20 \pm 0.10$, indicating that less than 1 dB additional noise cancellation is possible with a Wiener filter. The
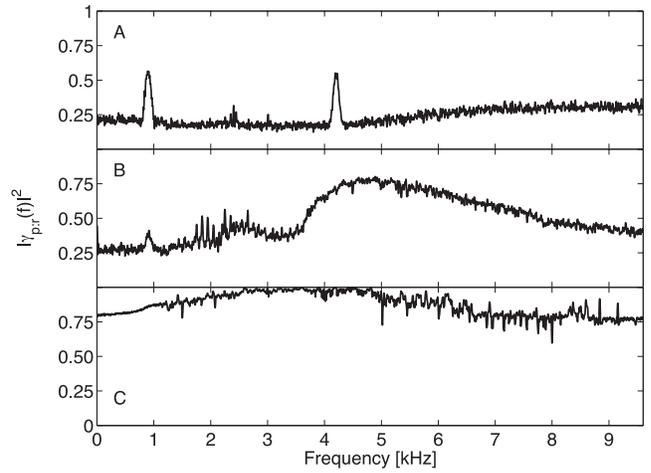
multiple coherence function is based on 32 stacked measurements. The standard deviation increases slightly outside the bandpass filter region due to the smaller amplitude of the signals here. Two broad peaks with an amplitude of 0.55 are seen at 900 and 4200 Hz in the coherence function. The nature of the noise causing these peaks is currently unknown, but is believed to be an instrumental artefact. The spectral densities at these frequencies are approximately 20 and 30 dB lower than the peak of the bandpass filter. Therefore, cancelling noise at these peaks will only have a minute effect on the retrieved FID curve. Finally, an important feature is found in a few small peaks with amplitude of approximately 0.25–0.30 located at powerline harmonic frequencies, most notably at 2400 and 3000 Hz. These peaks are attributed to an imperfect model-based removal of the powerline harmonics and an additional attenuation of up to 1.5 dB is theoretically possible at these frequencies. The likely explanation of the imperfect model-based removal of the powerline harmonics is that the fundamental powerline is changing so fast during the acquisition of a number of stacks that the assumption of a fixed frequency is only approximately true.

A second example is based on data recorded in Odder, 2 km away (Fig. 8b). This site is also rich in powerline interference and spikes. Close to the Larmor frequency, the multiple coherence function is above 0.30 ± 0.10 with peaks of 0.50 to 0.60 at some of the powerline harmonic frequencies. The measurement is based on averaging 50 stacks. These values of the multiple coherence function imply that the broad-band noise can be further suppressed by 1.5 dB and the imperfectly removed powerline harmonics can be reduced by an additional 3–4 dB.

The final example is from Kasted, 10 km west of Aarhus, Denmark (Fig. 8c). This site is very noisy and rich in powerline harmonics, but almost completely devoid of spikes. The absence of spikes is attributed to the fact that the data were recorded in January where thunderstorms are rare and most electrical fences are switched off. At this site, the multiple coherence function is remarkably high after model-based removal of powerline harmonics. In the interesting region around the expected Larmor frequency from 2 to 2.3 kHz, the mean value exceeds 0.93 ± 0.02. This high value of the multiple coherence implies that a further more than 11 dB additional noise attenuation is possible by a subsequent multichannel Wiener filter.

Table 1. Comparison of signal processing methods for Odder I (low multiple coherence) and Odder III, Kasted I and Kasted II (high multiple coherence). The synthetic signal has $s_0 = 200$ nV and $T_2^* = 75$ ms.

	s_0 (nV)	T_2^* (ms)	SNR
Odder I			
Pure stacking	178.9 ± 5.7	79.5 ± 5.1	0.3
Wiener filter	191.1 ± 1.9	73.4 ± 1.4	6.4
Model-based	188.3 ± 1.3	75.2 ± 1.1	25.1
Model-based and Wiener	185.5 ± 1.4	74.8 ± 1.2	26.9
Odder III			
Pure stacking	192.8 ± 21.9	96.1 ± 14.7	0.014
Wiener filter	207.2 ± 1.9	70.7 ± 0.9	1.36
Model-based	257.8 ± 11.4	68.4 ± 4.2	0.048
Model-based and Wiener	204.1 ± 2.3	74.6 ± 1.2	0.66
Kasted I			
Pure stacking	N.A.	N.A.	0.002
Wiener filter	175.2 ± 43.3	80.3 ± 39.8	0.021
Model-based	69.5 ± 39.3	286.6 ± 418.4	0.032
Model-based and Wiener	200.7 ± 18.6	70.0 ± 12.6	0.194
Kasted II			
Pure stacking	N.A.	N.A.	0.0007
Wiener filter	280.6 ± 3.8	51.2 ± 1.0	0.48
Model-based	277.4 ± 25.1	54.0 ± 6.9	0.016
Model-based and Wiener	232.5 ± 2.1	62.8 ± 0.8	1.21

5 COMPARISON OF NOISE CANCELLATION TECHNIQUES

To quantify the conclusions from the above sections, a number of numerical experiments have been carried out where a mono-exponential synthetic signal, eq. (10), has been embedded in the four different noise-only records from one site with low multiple coherence (Odder I) and three sites with high multiple coherence (Odder III, Kasted I and Kasted II). The parameters of the synthetic signal are $s_0 = 200$ nV, $T_2^* = 75$ ms, $f_L = 2075$ Hz and $\phi = 2$ rad. Four different noise cancelling methods are used and compared (Table 1). In all four methods, spikes have been removed from the records prior to further signal processing with the despiking method described in Dalgaard *et al.* (2012). The four methods are: (1) pure stacking, that is, plain averaging over the signal records, (2) multichannel Wiener filtering followed by stacking, (3) model-based removal of powerline harmonics followed by stacking and (4) model-based removal of powerline harmonics followed by multi-channel Wiener filtering and subsequent stacking. The multichannel Wiener filter is implemented in the frequency domain. Long signal records are used so that the transfer functions can be estimated on the last signal-free part of each signal record. This method helps to remedy the problem of jitter between the noise-only and signal records in the Numis Poly system (Dalgaard *et al.* 2012). The number of stacks employed is 32 for Odder I and 99 for the other sites.

The signal-to-noise ratio (SNR) is defined for the stacked records as

$$\mathrm{SNR} = \frac{\sum_k s^2(k)}{\sum_k n^2(k)}. \tag{12}$$

The noise $n(k) = x(k) - s(k)$ is found as the difference between the processed and stacked signal $x(k)$ and the synthetic signal $s(k)$. The SNR depends on the choice of synthetic signal and the summation limits for k as the MRS signal decays, while the noise is stationary. Here, the sum extends over the first 250 ms of the record. The model parameters are determined by envelope detection as described in Dalgaard *et al.* (2012) and fitting the envelope to the mono-exponential decay.

The noise at the site with low multiple coherence (Table 1, Odder I) is dominated by powerline harmonics. As expected pure stacking is the most inefficient method with a SNR of 0.3. However, the fitted parameters of the mono-exponential synthetic signal are still retrieved to with approximately 10 per cent. When Wiener filtering is employed, the SNR is increased to 6.4 and the model parameters are better determined. The SNR is increased fourfold to 25.1 by using model-based removal of powerline harmonics. However, the increase in SNR does not lead to a significantly improved determination of the model parameters. Finally, by combining the model-based approach with Wiener filtering, an additional small increase in SNR to 26.1 is gained, but again without a significant improvement in the fitted model parameters. Numerical experiments have shown that much larger increases in SNR are needed to significantly increase the determination of the model parameters.

The initial amplitude of the signal is underestimated with all four methods. This observation is partly explained by the interference from a non-stationary component of unknown origin at approximately 2000 Hz in the recordings. The component is unrelated to the powerline harmonics and only observed in the primary channel. Further signal processing can be used to remove this component and improve the signal.

The results from the high multiple coherence sites reflects the different noise environments at each specific site (Table 1, Odder III, Kasted I and II). At Odder III, the SNR is lower with all four methods than at Odder I and further, the SNR with Wiener filtering is higher than with model-based subtraction, in contrast to Odder I. Likewise, the retrieved model is badly determined using only model-based subtraction. This is caused by the more complex noise environment at this site, and hence removal of powerline harmonics alone is not enough to give an adequate noise cancelling. With the combined approach, the retrieved model is in good agreement with the synthetic model.

The noise levels at Kasted I and II are significantly larger than at the Odder sites and this is reflected in lower SNR. As above, pure stacking is the most inefficient method with a SNR of only 0.002 and 0.0007. These SNRs are so low that the mono-exponential signal cannot be reliably fitted. When Wiener filtering is employed, the SNR is greatly increased and the model parameters can be determined to within approximately 10 per cent for Kasted I and approximately 40 per cent for Kasted II. With the model-based approach, the SNR is also significantly increased, but the parameters of the mono-exponential decay are badly determined for Kasted I. For Kasted II, the results are similar to Wiener filtering. Finally, the combined model-based and Wiener filtering approach leads to improved SNR ratio and an adequate determination of the model parameters and their uncertainties.

From the above experiments, we conclude that the combined approach using first model-based powerline removal followed by multichannel Wiener filtering gives the best SNR and determination of the model parameters for all four sites. The exact increases in SNR are related to the noise characteristics at the specific site. For example, for Odder I where the main noise component is harmonic interference, the model-based approach by itself gives an adequate noise cancelling, whereas for Kasted where both harmonic and non-harmonic noise is present, the combined method must be used for good noise cancelling.

6 FULL SOUNDING EXAMPLE

In the above sections, a mono-exponential decay has been used for algorithm optimization for simplicity. In this section, synthetic signals are instead derived from a more realistic three-layer model and the comparison of different noise cancelling methods is performed on the retrieved model after inversion. The three-layer model has boundaries at 10 and 30 m and a water content of 5 per cent in the top layer, 30 per cent in the middle layer and 10 per cent in the bottom layer. The T_2^* model values are 150 ms in the top layer, 150 ms in the middle layer and 80 ms in the bottom layer. From this model, a forward response is calculated using Aarhus Inv (AAI; Behroozmand *et al.* 2012) and added to noise-only records from either the low-noise, low multiple coherence site at Odder or the high-noise, high multiple coherence site at Kasted. In both cases, we compare the three methods of multichannel Wiener filtering, model-based removal of powerline harmonics and the combined approach of first removing powerline harmonics followed by a subsequent multichannel Wiener filter. Subsequent to the noise cancelling, the model of the subsurface is obtained by inversion of the data using AAI.

For the low-noise site in Odder, a water content in good agreement with the synthetic model is found with all three noise cancelling methods (Fig. 9). The combined approach is slightly better than the two other approaches in estimating the water content in the top layer. For the T_2^* results, the combined approach also gives the best performance and in particular the top layer result is in good agreement with the model using this method, whereas T_2^* is overestimated using the other methods (Fig. 10). From a practical perspective, the fact that the model-based removal of harmonics alone gives good results implies that for sites known to be low in noise and dominated by powerline interference, good estimates of the layers and their water content can be obtained without deploying reference coils.

For the high-noise, high multiple coherence site at Kasted, a shortcoming of noise cancelling with multichannel Wiener filtering is observed. The depth of the lower boundary is in disagreement with the model and the water content is inadequately determined (Fig. 11a). The model-based harmonic subtraction performs better in determining both the depth of the boundaries and the water content (Fig. 11b). With the combined approach, a slightly better
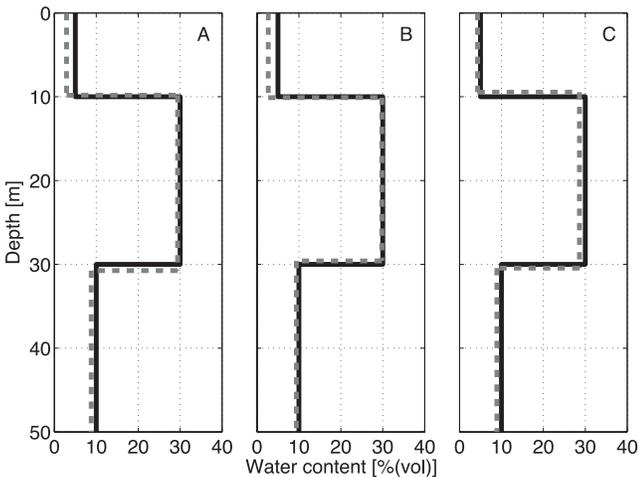
Figure 10. Inverted T_2^* values for a synthetic three-layer model (black), superimposed in noise-only records from the low-noise site at Odder. Grey lines show inverted models. (a) Multichannel Wiener filtering. (b) Model-based removal of harmonics. (c) Model-based and multichannel Wiener.
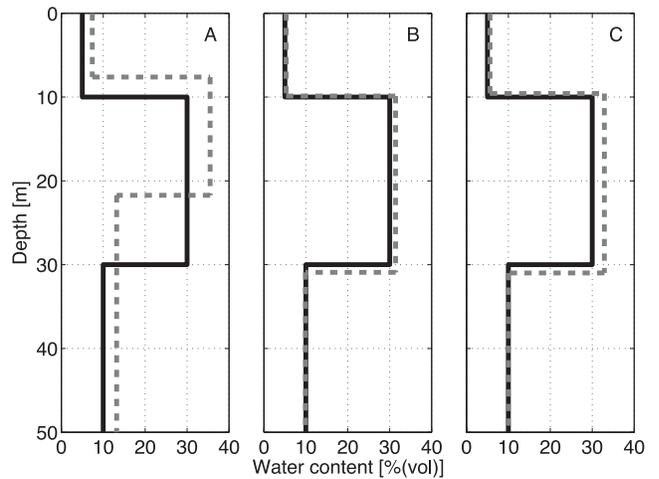
Figure 11. Inverted water content for the synthetic three-layer model (black) superimposed in noise-only records from the high-noise site at Kasted. Grey lines show inverted models. (a) Multichannel Wiener filtering. (b) Model-based removal of harmonics. (c) Model-based and multichannel Wiener.

agreement is obtained (Fig. 11c). The retrieved parameters are closer to their actual values and the residual error between the model and the data in the inversion is reduced. All three methods have problems in T_2^* in the top and middle layer at this site (Fig. 12). The results presented here are for one particular high-noise site. The results from other high-noise sites differ somewhat in the inverted models, but data from all investigated sites show that the combined approach gives the most accurate retrieval of the three-layer model.

7 CONCLUSION

We investigated the feasibility of an elaborate method of noise cancelling of MRS signal records. The method is based on utilizing the prior knowledge of the powerline harmonic noise component to model the noise and subtract the model from the records. We found that, once optimized, the approach is efficient in removing the powerline component from the records. Subsequently, standard multichannel Wiener filtering and averaging can be employed for

Figure 9. Inverted water content for a synthetic three-layer model (black), superimposed in noise-only records from the low-noise site at Odder. Grey lines show inverted models. (a) Multichannel Wiener filtering. (b) Model-based removal of harmonics. (c) Model-based and multichannel Wiener.
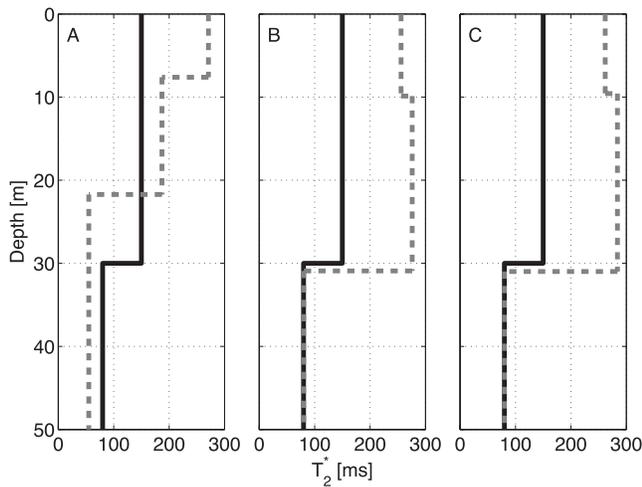
Figure 12. Inverted T_2^* values for a synthetic three-layer model (black), superimposed in noise-only records from the low-noise site at Odder. Grey lines show inverted models. (a) Multichannel Wiener filtering. (b) Model-based removal of harmonics. (c) Model-based and multichannel Wiener.

further noise reduction. The method typically adds a few hours of computational work in the post-processing of the data.

The efficiency of the method depends on the exact distribution between different noise sources at the site of measurement. If the specific site is completely dominated by one noise source, a multichannel Wiener filter can be adequate, but when the noise distribution is more complex, it is better to remove powerline harmonics with the model-based approach before further noise cancelling by multichannel Wiener filtering is employed. However, it is important to stress that the problem of multiple noise sources still remains. The method proposed here only solves one part of the problem by removing the specific noise component consisting of powerline interference. Further, the method is based on the assumption that the powerline frequency remains stable through the recording of each stack. If this assumption is invalid, the efficiency of the method is decreased.

Our previous results on optimization of noise cancelling were limited by jitter and uneven sampling frequencies in the primary and reference channels in the recording apparatus. Modelling of powerline harmonics partly removes this problem as the harmonic noise is independently processed and removed for each channel.

For the Numis Poly system, the acquisition time increases with the number of channels used. In practice, sometimes, fast measurements are necessary and reference coils are therefore not deployed with a corresponding reduction in data quality. In such cases, model-based removal of the powerline harmonics can help in increasing the data quality.

The first experimental results indicate that the method allows us to do square-loop configuration measurements on sites where high levels of noise previously warranted a figure-8 configuration. As the figure-8 configuration reduces depth penetration and is more cumbersome to deploy in the field, this method can potentially increase the applicability of the MRS technique. This hypothesis will be investigated in future work.

We tested the method on data recorded in Denmark where all powerline harmonics are multiples of the fundamental 50 Hz frequency. The method should be equally useful in countries with 60 Hz power grids and in countries where electrical trains run on subharmonics such as $16\frac{2}{3}$ Hz by simple extensions of the modelling methods. This work has only dealt with the problem of estimating initial amplitudes and decay times, but can also be extended towards spin-echo measurements.

ACKNOWLEDGEMENTS

REFERENCES

Behroozmand, A., Auken, E., Fiandaca, G., Christiansen, A.V. & Christensen, N.B., 2012. Efficient full decay inversion of MRS data with a stretched-exponential approximation of the T_2^* distribution, *Geophys. J. Int.,* **190,** 900–912.

Bendat, J.S. & Piersol, A.G., 2010. *Random Data, Analysis and Measurement Procedures,* 4th edn, Wiley.

Butler, K.E., 2001. Comment on design of a hum filter for suppressing power-line noise in seismic data, *J. Environ. Eng. Geophys.,* **6**(2), 103–104.

Butler, K.E. & Russell, R.D., 1993. Subtraction of powerline harmonics from geophysical records, *Geophysics,* **58**(6), 898–903.

Butler, K.E. & Russell, R.D., 2003. Cancellation of multiple harmonic noise series in geophysical records, *Geophysics,* **68**(3), 1083–1090.

Dalgaard, E., Auken, E. & Larsen, J.J., 2012. Adaptive noise cancelling of multichannel magnetic resonance sounding signals, *Geophys. J. Int.,* **191,** 88–100.

Dlugosch, R., Mueller-Petke, M., Günther, T., Costabel, S. & Yaramanchi, U., 2011. Assessment of the potential of a new generation of surface nuclear magnetic resonance instruments, *Near Surf. Geophys.,* **9,** 89–102.

Lay, D.C., 2012. *Linear Algebra and its Applications,* 4th edn, Pearson.

Legchenko, A. & Valla, P., 2003. Removal of power-line harmonics from proton magnetic resonance sounding measurements, *J. appl. Geophys.,* **53,** 103–120.

Legchenko, A., Baltassat, J.-M., Beauce, A. & Bernard, J., 2002. Nuclear magnetic resonance as a geophysical tool for hydrogeologists, *J. appl. Geophys.,* **50,** 21–46.

Mueller-Petke, M. & Yaramanci, U., 2010. Improving the signal-to-noise ratio of surface-NMR measurements by reference channel based noise cancellation, in *Proceedings of the Near Surface 2010, 16th European Meeting of Environmental and Engineering Geophysics,* Zurich, Switzerland.

Walsh, D.O., 2008. Multi-channel surface NMR instrumentation and software for 1D/2D groundwater investigations, *J. appl. Geophys.,* **66,** 140–150.

Xia, J. & Miller, R.D., 2000. Design of a hum filter for suppressing power-line noise in seismic data, *J. Environ. Eng. Geophys.,* **5**(2), 31–38.